Molecular Dynamics Simulation of a Rhinovirus Capsid under Rotational Symmetry Boundary Conditions

SHIGETAKA YONEDA,* MASAKO KITAZAWA, and HIDEAKI UMEYAMA

School of Pharmaceutical Sciences, Kitasato University, 5-9-1 Shirokane, Minato-Ku, Tokyo 108, Japan

Received 28 February 1994; accepted 8 May 1995

ABSTRACT

The rotational symmetry boundary condition proposed by Cagin et al. [*J. Comp. Chem.*, **12**, 627 (1991)] is implemented in the molecular dynamics simulation program, APRICOT, to make simulations of icosahedrally symmetrical capsids practical. The principle of the rotational symmetry boundary condition is strictly formulated with a new algorithm to track each atom by protomer and cell number. Further, the 60 cells and the 60 protomers of a capsid are treated as elements of the point group I. This treatment is necessary to determine the protomer numbers of atoms and to define indicators of atom pairs named relative protomer numbers. A method designated border residue flags is also introduced to further accelerate neighbor atom pair list generation. The method as we have implemented it is so fast that it was possible, using inexpensive workstations, to perform a 60-ps molecular dynamics simulation on an entire structure of a rhinoviral capsid including a 71-Å-thick shell of water molecules. This work is the first molecular dynamics simulation of an entire capsid under rotational symmetry boundary conditions. The structure of the capsid is well conserved during the simulation. Because conventional periodic boundary conditions are not applicable to rotational symmetries, it has been difficult, until this study, to perform calculations on macromolecules in crystallographic or noncrystallographic symmetries that are composed of rotational symmetries and linear translation. Therefore, our development is expected to provide a powerful tool for studies of macromolecules in such symmetries. The merits, limitations, and possibilities for further elaboration of this development are discussed.

*Author to whom all correspondence should be addressed at School of Science, Kitasato University, 1-15-1 Kitasato, Sagamihara-Shi, Kanagawa-Ken 228, Japan.

Journal of Computational Chemistry, Vol. 17, No. 2, 191–203 (1996)

CCC 0192-8651 / 96 / 020191-13

Introduction

Viruses have intrigued biological and chemical scientists both as one of the mysteries of life and as serious causative agents in human disease. X-ray analyses have been performed for many viral protein shells, known as capsids. The capsid is a multifunctional container that not only carries the viral genome, but also is able to escape immunological attack, to infect host cells, and to leave the cell after viral multiplication. With the X-ray coordinates of capsids, such elaborate mechanisms can, in principle, be investigated at the atomic level by computational chemistry methods, especially molecular dynamics simulation.

However, viral capsids are too large for direct simulation. For example, the capsid of a rhinovirus (a typical small virus) has 500,000 atoms, and its diameter is 300 Å.[1] Conventional molecular dynamics simulations of the entire capsid are therefore not practical. Fortunately, viral capsids are generally assemblies of many identical copies of a protomer (molecular unit), the spatial arrangement of which is helical, icosahedral, or a combination of both types of symmetry.[2] In this article, we take the well-defined X-ray coordinates[1] of a rhinoviral capsid with icosahedral symmetry and present a molecular dynamics simulation using symmetry constraints.

Icosahedral symmetry is a three-dimensional rotational symmetry (point group I), such that the 60 protomers are related to each other by 60 rotational transformations around six fivefold axes, 10 threefold axes, and 15 twofold axes.[2] The X-ray coordinates of the rhinoviral capsid were determined from a cubic crystal with $P2_13$ symmetry.[1] A unit cell of that crystal contains four capsids in the $P2_13$ symmetry, and each of these four contains 60 protomers in icosahedral symmetry.

If icosahedral symmetry is assumed, a capsid calculation is restricted to one sixtieth of the entire capsid structure. Energy calculation involving bond lengths, bond angles, and torsional angles will then be as fast as in an isolated protomer calculation. Furthermore, the nonbonded interaction calculation will also be nearly as fast as in an isolated protomer calculation, if the neighbor atom pair list is already generated and the nonbonded interaction is truncated at a reasonable cutoff distance R_c. For example, the traditional R_c of 8 Å is much smaller than the protomer size, so the number of atoms encompassed by a sphere of radius R_c is small compared to the number of atoms within the protomer itself. Consequently, central processing unit (CPU) time for calculation of the nonbonded energy is not excessively different from that required for an isolated protomer calculation. However, generation of the neighbor list still consumes a lot of CPU time. If the number of the protomer atoms is N, approximately $N^2/2$ atom pair distance calculations (when N is very large) are necessary for neighbor list generation in an isolated protomer calculation. On the other hand, when icosahedral symmetry is assumed, any atom of a protomer may interact not only with atoms of that protomer, but also with those of any of the other 59 protomers. Therefore, calculations of approximately $(N^2/2) + 59 \cdot N^2$ atom pair distances are necessary for neighbor list generation. Neighbor list generation for icosahedral symmetry takes about $\{(N^2/2) + 59 \cdot N^2\}/(N^2/2) = 119$ times more CPU time than in an isolated protomer calculation.

Cagin, Holder, and Pettitt first proposed rotational symmetry boundary conditions[3] (i.e., calculations to be carried out for the molecular structure within a computational cell). The computational cell proposed by Cagin et al. (shown in Fig. 1a) is a typical asymmetrical unit of icosahedral symmetry. The computational cell is not equivalent to a crystal cell or lattice, although the same name *cell* is used. We hereafter use the word *cell* as an abbreviation of *computational cell* according to convention. Although *box* is also used sometimes instead in periodic boundary condition studies, this is not appropriate for the shape shown in Figure 1a.

The whole three-dimensional space is divided into 60 cells. The molecular structure within a cell is composed of partial structures of several protomers. Thus, a single protomer is contained within several cells. The cell for which calculations are performed is named the central cell. Because the shape of the defined cell is simple, atoms in the central cell can interact with only the eight surrounding cells or the central cell itself, as long as R_c is less than the shortest cell width of about 35 Å (Fig. 1b). Consequently, neighbor list generation under rotational symmetry boundary conditions will take only about $(N^2/2) + 8 \cdot N^2$ atom pair distances and therefore will require only about $\{(N^2/2) + 8 \cdot N^2\}/(N^2/2) = 17$ times the CPU time required for an isolated protomer calculation. Thus the rotational symmetry boundary condition

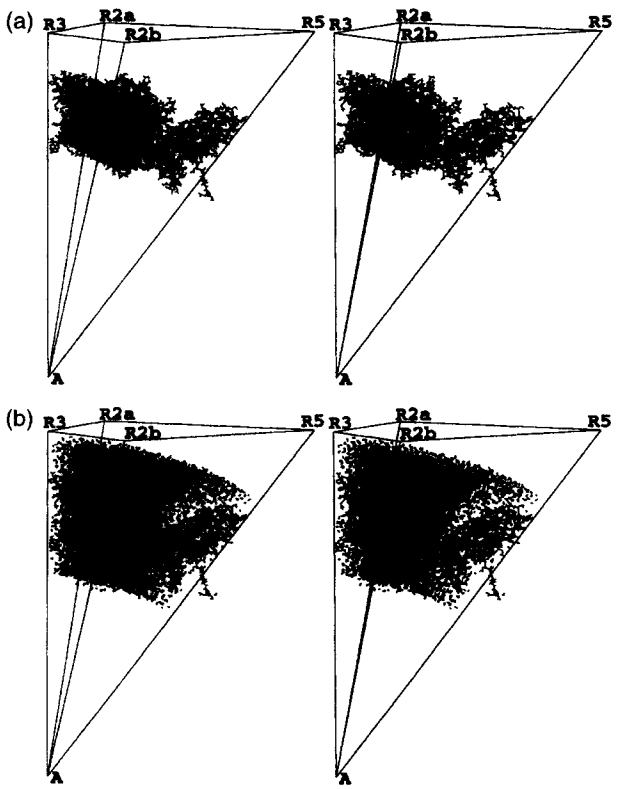

FIGURE 1. Stereoview of the rhinovirus capsid structure energy minimized under rotational symmetry boundary conditions. The letter A denotes the center of symmetry. The lines A-R5 and A-R3 denote fivefold and threefold axes of icosahedral symmetry, respectively. The lines A-R2a and A-R2b denote twofold axes of icosahedral symmetry. The cell is a space surrounded with the edge lines of A-R5, A-R3, A-R2a, and A-R2b. The cage depicts the cell truncated with the icosahedral surface. The length of A-R3 is 170 Å. The protein shown is not the cell structure but the protomer structure. (a) Water molecules not shown. (b) Water molecules shown. Water molecules are distributed in the water zone defined in the text, with inner radius of 99 Å and outer radius of 170 Å. The outer surface of the zone is a spherically curved quadrangle, two sides of which have length of 61.7 Å; the other two are 92.9 Å. The inner surface is also a spherically curved quadrangle, two sides of which have length of 35.9 Å; the other two are 54.1 Å. Thus, the shortest width of the water zone is 35.9 Å, and if the cutoff distance R_c < 35.9 Å is used, the intercell interaction is contributed only by neighboring cells.

proposed by Cagin et al. can marvelously accelerate neighbor list generation for capsid calculations.

The molecular structure within the central cell is made by rotation of atoms of a protomer as follows:

$$\mathbf{x}(k') = \mathbf{R}[m] \cdot \mathbf{x}(k) \qquad (1)$$

where $\mathbf{R}[m]$ is one of the 60 rotation matrices of icosahedral symmetry. The coordinates of atom k, $\mathbf{x}(k)$, move to the coordinates of atom k of another protomer, $\mathbf{x}(k')$. Selecting $\mathbf{R}[m]$ appropriately, it is possible to locate $\mathbf{x}(k')$ in the central cell. Applying such rotations to all the atomic coordinates of a protomer, it is possible to make the molecular structure within the central cell. This operation proposed by Cagin et al.,[3] which we refer to as the packing operation, is a basis of the rotational symmetry boundary condition.

A similar operation is sometimes carried out for calculations in periodic boundary conditions, using the following minimum image convention[4]:

$$\mathbf{V}' = \mathbf{V} - [\mathbf{V}/L + 0.5] \cdot L \qquad (2)$$

where L is the length of periodicity and $\mathbf{V}$ and $\mathbf{V}'$ are vectors. For simplicity, we present the one-dimensional form. The symbol [ ] is the so-called Gauss symbol (i.e., $[x]$ presents the largest integer which is smaller than x). For example, $[1.23] = 1$ and $[-3.42] = -4$. With eq. (2), any vector $\mathbf{V}$ moves to its shortest image $\mathbf{V}'$. If eq. (2) is applied to atomic position vectors, atoms move into the periodic boundary box nearest to the origin (i.e., the atoms move into the interval of $(-L/2, L/2)$ in one-dimensional space). Generally, in molecular dynamics calculations of liquids and gases, atoms are highly mobile and are often dispersed from the initial positions into other boxes as simulation proceeds. Thus, packing the atomic distribution with eq. (2) is a useful technique to make clearer animations of liquids and gases.

However, such packing is not essential to the principle of the periodic boundary condition.[4] Generally, if periodicity is assumed, an atom i may interact not only with another atom j, but also with atom j's infinitely many images. Among these images, the nearest one to atom i is expected to make the largest interaction with atom i. Further, if a cutoff distance, R_c, is selected shorter than length of periodicity (i.e., $R_c < L$), all images except the nearest image can be neglected in energy calculations. Thus, determining the nearest image is the most basic function for the periodic boundary conditions. However, distance calculations to determine the nearest image are not possible because atom j's images are infinitely many. However, if eq. (2) is applied to the relative vector between atoms i and j, the shortest relative image vector is obtained without distance calculations, and thus the position of atom j's image nearest to atom i is determined. Because eq. (2) consumes

little CPU time, it is possible to insert eq. (2) in all energy subroutines and to replace all kinds of the relative vectors with their shortest image vectors. Periodicity is implicitly treated. This is the principle of the periodic boundary condition.[4] Even if the atomic distribution is dispersed as the simulation proceeds, results of eq. (2) are not affected. Thus the packing of atomic positions is not essential to the periodic boundary conditions.

The preceding minimum image convention is not applicable to rotational symmetry. Even if eq. (1) is applied to a relative vector, no shortest image vector is obtained. Furthermore, eq. (1) includes a complicated matrix rotation and consumes much CPU time. Thus, it would be difficult to insert eq. (1) in all energy subroutines. Furthermore, if atoms i and j are near a symmetry axis, several images of atom j are also near the axis, and many of them may be within a cutoff distance from atom i. Thus, to determine which images are within the cutoff, distance calculations for many images are inevitable. Consequently, rotational symmetry cannot be considered implicitly. The key idea behind the rotational symmetry boundary condition is to accelerate generation of neighbor lists with the packing operation, and therefore this condition is much different from the principle of the periodic boundary condition.

The molecular structure made by the packing operation is a combination of atoms of several protomers. Two of atoms within a cell are not necessarily of the same protomer. If the atoms are of different protomers, no bond would be possible between the atoms (except interprotomer disulfide bonds). Thus, for calculations in rotational symmetry boundary conditions, it is necessary to determine whether atoms are of the same protomer. A new method is therefore necessary to determine the protomer numbers of atoms within a cell. Furthermore, a method to describe the relationship of the protomer numbers of atom pairs is also necessary. Previously, simulation of viral capsids has been restricted to a single protomer with a small portion of those surrounding it[5-7] or to a single protomer without interprotomer interactions.[8] Although symmetry constraints are easily applied in molecular dynamics simulations,[9] practical calculations in rotational symmetry boundary conditions are not easy. Calculations of capsids presented by Cagin, Holder, and Pettitt were restricted to a minimization with the conventional replication method.[3]

In this article, we first propose to use subscripts and superscripts to indicate the protomer numbers and the cell numbers of atoms, respectively. Using this notation, the 60 images of an atom in icosahedral symmetry are differentiated, and the principle of the rotational symmetry boundary condition is strictly formulated. Further, we develop a notation to treat the 60 cells and the 60 protomers as elements of the point group I. Using these, we develop equations to determine protomer numbers of atoms and define relative protomer numbers of atom pairs. Additionally, a new method named border residue flags is developed to accelerate neighbor list generation. A 60-ps molecular dynamics simulation of a rhinoviral capsid is presented using these developments. This is the first practical simulation of an entire capsid structure using rotational symmetry boundary conditions. Although the methods are applicable for other types of symmetry, the following descriptions are restricted to the case of icosahedral symmetry.

Methods

A STRICT FORMULATION OF THE ROTATIONAL SYMMETRY BOUNDARY CONDITION

To identify an atom in a capsid, we propose a notation using a combination of two numbers denoted, k_p, where k is the sequential atom number defined in a protomer and the subscript p is the protomer number. Another notation, k^c, can also be used where the superscript c is the cell number. With either k_p or k^c, any atom of a capsid can be uniquely identified.

All the cells are numbered from 0 to 59. The central cell is numbered zero, and the neighboring cells are numbered from 1 to 8. The protomers are numbered according to the cell numbers: If the largest part of a protomer is contained in a cell numbered n, then the number of that protomer is defined as n. We refer to the protomer numbered zero as the central protomer. The central protomer is the protomer which occupies the largest part of the central cell.

A more strict definition is necessary for the rotation matrix **R**, which appeared in eq. (1). We define **R**[m] as a rotation matrix with which the central cell is rotated onto cell m, as follows:

$$\mathbf{x}(k^m) = \mathbf{R}[m] \cdot \mathbf{x}(k^0) \qquad (3)$$

where $\mathbf{x}(k^m)$ and $\mathbf{x}(k^0)$ are the coordinates of atoms in cell m and in the central cell, respectively. For example, with matrix **R**[0], the central cell moves

to the central cell itself. With **R**[1], the central cell moves to cell 1. With **R**[2], the central cell moves to cell 2, etc. Using eq. (3), each of the 60 rotation matrices uniquely corresponds to one of the 60 cells. Similarly, each rotation matrix also uniquely corresponds to one of the 60 protomers, using the following equation:

$$\mathbf{x}(k_m) = \mathbf{R}[m] \cdot \mathbf{x}(k_0) \qquad (4)$$

where $\mathbf{x}(k_m)$ and $\mathbf{x}(k_0)$ are the coordinates of atoms of protomer m and of the central protomer, respectively. We write the inverse matrix of $\mathbf{R}[m]$ as $\mathbf{R}[-m]$. With $\mathbf{R}[-m]$, cell m moves to the central cell, and protomer m moves to the central protomer. The 60 rotation matrices make the point group I of icosahedral symmetry and satisfy the rules of the group theory.

We introduce a function, $\mathrm{cl}(k_p)$, to indicate the cell number where atom k_p is located. Because all the 60 cells are separated with 15 symmetry planes, $\mathrm{cl}(k_p)$ can be determined from the position of atom k_p relative to those 15 planes. In this study, however, only nine cells are considered so that the relative positions to the seven planes, as shown in Figure 2, are necessary and sufficient. For example, when an atom is above planes 1, 5, 6, and 7 and below planes 2 and 3, the atom is within the cell 1. Table I shows the relationship between $\mathrm{cl}(k_p)$ and the relative position to the partition planes.

Using the preceding notations and function, the packing operation of eq. (1) can be more strictly formulated as follows:

$$\mathbf{x}(k^0) = \mathbf{R}\left[-\mathrm{cl}(k_p)\right] \cdot \mathbf{x}(k_p) \qquad (5)$$

From definition of the rotation matrices, the matrix, $\mathbf{R}[-\mathrm{cl}(k_p)]$, is the rotation matrix to move the cell where atom k_p is located onto the central cell. Thus, atom k_p moves into the central cell with this rotation matrix. If eq. (5) is applied to all the atoms of a protomer, atomic coordinates of the central cell are generated. Consequently, by combination of the packing operation [eq. (5)] and rotation [eq. (3)], any cell coordinates can be generated from the coordinates of a protomer. In contrast, the principle of rotational symmetry boundary conditions proposed by Cagin et al. was to perform energy calculations by using $\mathbf{x}(k^c)$ instead of $\mathbf{x}(k_p)$.

CELLS AND PROTOMERS TREATED AS THE POINT GROUP I

It is usual to write a product of two matrices $\mathbf{R}[m]$ and $\mathbf{R}[n]$ as $\mathbf{R}[m] \cdot \mathbf{R}[n]$. For example, $\mathbf{R}[2] = \mathbf{R}[2] \cdot \mathbf{R}[0]$ and $\mathbf{R}[1] = \mathbf{R}[2] \cdot \mathbf{R}[2]$ (see Fig. 2). Because the symbols **R**[ ] look superfluous, we introduce symbols $\equiv$ and $\oplus$. For example, the preceding equations are written as $2 \equiv 2 \oplus 0$ and $1 \equiv 2 \oplus 2$, respectively. Further, **R**[2] and **R**[1] can be written as **R**[2 ⊕ 0] and **R**[2 ⊕ 2], respectively. If values of $m \oplus n$ are generated for all combinations of m and n, the resulting multiplication table defines the mathematical property of the point group I of icosahedral symmetry.

Because eq. (4) establishes the unique correspondence between rotation matrices and protomer numbers, the protomers compose the point group I which is isomorphic to the group of the rotation matrices. We also use the notations of $\equiv$

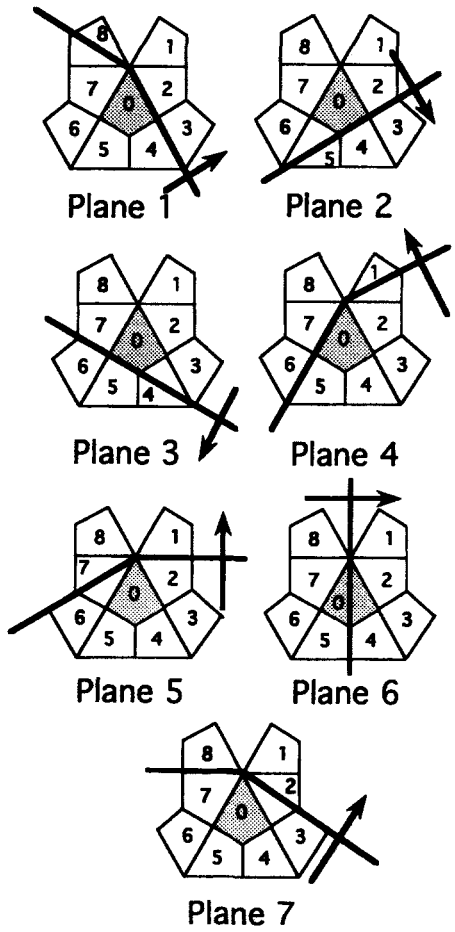

FIGURE 2. The nine cells and the seven partition planes. The central cell is numbered 0. Only eight cells share edges with the central cell. The planes are drawn in bold lines, and the arrows denote the upward directions of the planes. The figure is an expansion of the icosahedral surface onto a plane, so some lines are bent.

TABLE I.
Relationship between cl(k_p) and the Position of Atom k_p Relative to the Partition Planes.

Plane 7	Plane 6	Plane 5	Plane 4	Plane 3	Plane 2	Plane 1	Cell Number
0	0	0	0	0	0	0	0
0	1	0	0	0	0	0	0
1	1	1	1	0	0	1	1
1	1	1	0	0	0	1	1
1	1	0	0	0	0	1	2
0	1	0	0	0	0	1	2
0	1	0	0	0	1	1	3
0	1	0	0	0	1	0	4
0	1	0	0	1	1	0	4
0	0	0	0	1	1	0	5
0	0	0	0	1	0	0	5
0	0	0	1	1	0	0	6
0	0	0	1	0	0	0	7
0	0	1	1	0	0	0	7
1	0	1	1	0	0	0	8
1	0	1	1	0	0	1	8

Numbers 1 and 0 represent the upward and the downward directions of the partition planes, respectively. Combinations which are not included represent the cells other than those numbered 0 to 8.

and $\oplus$ for the group of the protomers. Although multiplication of protomers may sound curious, definition of multiplication is possible for protomers, using the multiplication table of the rotation matrices. For example, we assume that the protomer numbers should satisfy an equation $1 \equiv 2 \oplus 2$, corresponding to the equation of the rotation matrices, $\mathbf{R}[1] = \mathbf{R}[2] \cdot \mathbf{R}[2]$. Treating the protomers as elements of the point group I is necessary for strict description of the relationship of protomer positions.

Similarly, because the 60 cells also uniquely correspond to the rotation matrices with eq. (3), the cells can be treated as elements of the point group I. The notation of $\equiv$ and $\oplus$ is applicable to the cell numbers, too.

PROTOMER NUMBER EQUATIONS OF ATOMS

With matrix $\mathbf{R}[p]$, atom k_0 of the central protomer moves to atom k_p of protomer p [eq. (4)]. With matrix $\mathbf{R}[-\mathrm{cl}(k_p)]$, this atom, k_p, moves to atom k^0 in the central cell [eq. (5)]. With $\mathbf{R}[c]$, this central cell atom, k^0, moves to atom k^c in cell c [eq. (3)]. Therefore,

$$\mathbf{x}(k^c) = \mathbf{R}[c] \cdot \mathbf{R}\left[-\mathrm{cl}(k_p)\right] \cdot \mathbf{R}[p] \cdot \mathbf{x}(k_0) \quad (6)$$

The preceding equation indicates that atom k_0 of the central protomer moves to atom k^c with the rotation matrix, $\mathbf{R}[c] \cdot \mathbf{R}[-\mathrm{cl}(k_p)] \cdot \mathbf{R}[p]$. Therefore, from the definition of protomer numbers [eq. (4)], the protomer number of atom k^c should be as follows:

$$\mathrm{pr}(k^c) \equiv c \oplus \left(-\mathrm{cl}(k_p)\right) \oplus p \quad (7)$$

where the function $\mathrm{pr}(k^c)$ presents the protomer number of atom k^c. When p is equal to 0, the preceding equation is

$$\mathrm{pr}(k^c) \equiv c \oplus (-\mathrm{cl}(k_0)) \quad (8)$$

The preceding equation is necessary to determine the protomer numbers of atoms for calculations in rotational symmetry boundary conditions. Furthermore, because an equation $c = \mathrm{cl}(k_p)$ is equivalent to $p = \mathrm{pr}(k^c)$, the two kinds of notations k_p and k^c are interchangeable with the functions $\mathrm{cl}(k_p)$ (Table I) and $\mathrm{pr}(k^c)$ [eq. (7) or (8)].

PROTOMER NUMBER EQUATIONS OF ATOM PAIRS

With rotation matrix $\mathbf{R}[m]$, atom i_p moves to its image, $i_{m\oplus p}$, and atom j_q moves to its image, $j_{m\oplus q}$ [eq. (4)]. Consequently, with this rotation matrix, an atom pair, (i_p, j_q), moves to $(i_{m\oplus p}, j_{m\oplus q})$. Thus, atom pair $(i_{m\oplus p}, j_{m\oplus q})$ is an image of (i_p, j_q). Atom pair (i_p, j_q) has 60 images in icosahedral symmetry: (i_p, j_q) itself, $(i_{1\oplus p}, j_{1\oplus q})$, $(i_{2\oplus p}, j_{2\oplus q})$,

$(i_{3\oplus p}, j_{3\oplus q}), \ldots,$ and $(i_{59\oplus p}, j_{59\oplus q})$. However, for example, $(i_{1\oplus p}, j_{2\oplus q})$ is not an image of (i_p, j_q). We name $q \oplus (-p)$ as the relative protomer numbers of atom pair (i_p, j_q). All 60 images of (i_p, j_q) have the same relative protomer numbers. Otherwise, they are not images of (i_p, j_q). Generally, $60 \times 60 = 3600$ combinations (i_s, j_t) are possible for the fixed atom numbers i and j. These 3600 atom pairs can be divided into 60 groups, each of which is composed of the 60 atom pairs with the same relative protomer numbers.

If atom pair (i_p, j_q) is bonded by a covalent bond, all of its 60 images should also be bonded. Thus, in icosahedral symmetry, a bond pair can be written as a triplet composed of two atom numbers and the relative protomer numbers, like $(i, j, q \oplus (-p))$.

In rotational symmetry boundary conditions, calculations are based on the cell coordinates. Thus, a method to determine the relative protomer numbers is necessary for pairs of the cell atoms. The relative protomer numbers of atom pair (i^c, j^d) is $\mathrm{pr}(j^d) \oplus (-\mathrm{pr}(i^c))$. Thus, from eq. (8),

$$\begin{aligned} &\mathrm{pr}(j^d) \oplus (-\mathrm{pr}(i^c)) \\ &\quad \equiv \{d \oplus (-\mathrm{cl}(j_0))\} \oplus \{-(c \oplus (-\mathrm{cl}(i_0))\} \\ &\quad \equiv d \oplus (-\mathrm{cl}(j_0)) \oplus \mathrm{cl}(i_0)) \oplus (-c) \end{aligned} \tag{9}$$

If the first atom i_c is assumed as the central cell atom (i.e., $c \equiv 0$), the preceding equation becomes

$$\mathrm{pr}(j^d) \oplus (-\mathrm{pr}(i^0)) \equiv d \oplus (-\mathrm{cl}(j_0)) \oplus \mathrm{cl}(i_0) \tag{10}$$

It is rare that a viral capsid has interprotomer disulfide bonds, and the first atom and the second atom of a bond pair usually have the same protomer number. If interprotomer bonds are not considered, bond pairs must satisfy $\mathrm{pr}(j^d) \oplus (-\mathrm{pr}(i^0)) \equiv 0$. Therefore, from eq. (10),

$$d \oplus (-\mathrm{cl}(j_0)) \oplus \mathrm{cl}(i_0) \equiv 0 \tag{11}$$

Rearranging,

$$d \equiv (-\mathrm{cl}(i_0)) \oplus \mathrm{cl}(j_0) \tag{12}$$

If this equation is satisfied, atoms i^0 and j^d are of the same protomer. The values of $(-\mathrm{cl}(i_0)) \oplus \mathrm{cl}(j_0)$ are given in Table II. Whether atom pairs are bonded or not is fundamental information for the molecular structure. This information is not only necessary for calculations of energy of bonds, angles, dihedrals, etc., but also for calculations of nonbonded interactions, because bonded atom pairs must be correctly excluded from the nonbonded interactions. Thus, eqs. (10), (11), and (12) enable correct differentiation of images of atom pairs and correct energy calculations in rotational symmetry boundary conditions.

TABLE II.
Values of $(-\mathrm{cl}(i_0)) \oplus \mathrm{cl}(j_0)$.

	$cl(j_0)$								
$cl(i_0)$	0	1	2	3	4	5	6	7	8
0	0	1	2	3	4	5	6	7	8
1	8	0	7	*	*	*	*	1	2
2	7	2	0	5	6	*	*	8	1
3	3	*	4	0	2	*	*	*	*
4	5	*	6	7	0	4	*	*	*
5	4	*	*	*	5	0	2	3	*
6	6	*	*	*	*	7	0	5	*
7	2	8	1	*	*	3	4	0	7
8	1	7	8	*	*	*	*	2	0

Asterisks represent protomers other than the nine protomers 0 to 8.

BORDER RESIDUE FLAGS

Seven boundaries were defined for a cell as shown in Figure 3, comprising four planar regions and three axes. Through these seven boundaries, a cell contacts other cells. For example, the central cell contacts cell 2 through its boundary 1, whereas cell 2 contacts the central cell through its boundary 4. The contacting boundary numbers are summarized in Table III.

As long as nonbonded interactions are truncated at some reasonable value of R_c ($R_c < \tau$, where τ is about 35 Å for the rhinoviral capsid, as

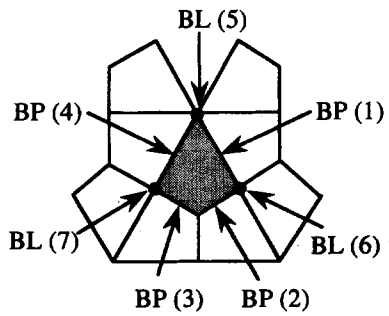

FIGURE 3. Seven boundaries of a cell. BP and BL denote the boundary planar regions and the boundary lines, respectively. Numbers in parentheses denote sequential numbers of the boundaries.

TABLE III.
Contacting Boundary Numbers.

Boundary A of the Central Cell Contacts
Boundary B of Cell c.

	Cell Number c							
	1	2	3	4	5	6	7	8
Boundary number B	5	4	6	3	2	7	1	5
Boundary number A	5	1	6	2	3	7	4	5

explained in Fig. 1), the intercell nonbonded interaction contribution comes only by residues located near the boundaries. For example, the nonbonded interaction between the central cell and cell 2 is contributed by residue pairs (a, b), of which residue a is in the central cell and near boundary 1 and residue b is in cell 2 and near boundary 4. We introduce an algorithmic device called border residue flags brf(a, k), where a is the residue number and k is the boundary number. If a residue a is near boundary k, then brf(a, k) is set on; otherwise brf(a, k) is set off. A special cutoff length, called border cutoff, is introduced as a criterion of nearness. The border cutoff must be longer than the cutoff of the nonbonded interaction. If the candidate atom pairs for the neighbor list generation are limited by the border residue flags, the number of distance calculations can be greatly decreased, thereby accelerating neighbor list generation.

The development in this section was implemented using the program APRICOT,[10] and molecular dynamics calculations of a rhinoviral capsid were carried out under rotational symmetry boundary conditions, as presented in the following sections. The nonbonded interactions were calculated using $\mathbf{x}(k^c)$; whereas the energies of bonds, angles, and dihedrals were calculated with the conventional method using $\mathbf{x}(k_p)$ because use of rotational symmetry boundary conditions does not accelerate energy calculations of bonds, angles, or dihedrals.

Computational Procedure

The initial atomic coordinates for the rhinoviral capsid calculations were taken from the X-ray coordinates, 4RHV.[1] A protomer of the rhinoviral capsid is composed of four peptide chains, VP1, VP2, VP3, and VP4, all of which have Swiss roll folds,[1,2] except the shortest strand VP4. The 4RHV file does not contain the coordinates of the amino termini of VP1, VP2, and VP4 due to disorder in the crystal. The amino termini were capped with acetyl groups, designated ACE in the input data, in the trans conformation. Other amino and all carboxyl termini were assumed to be charged. All histidine residues were assumed to be protonated at ND1. Explicit hydrogen atoms were added to the protein with standard bond lengths and angles. The AMBER united atom force field[11] for proteins and the TIP3P potential for water[12] were used. A residue-based cutoff[13] of 8 Å was adopted, and the neighbor list was updated every 20 steps. The coordinates of water molecules are also contained in the 4RHV file, and all of them were included for the calculations with the exception of the three water molecules HOH-1, HOH-66, and HOH-228, which were omitted (as discussed later).

Energy of the initial protomer structure was minimized by the conjugate gradient method, with a positional constraint force constant of 1000 kcal mol^{-1} $Å^{-2}$ applied to all the nonhydrogenic atoms except those of the acetyl groups. The dielectric constant used was 4.0. Minimization continued until the root mean square (rms) gradient became 0.6 kcal mol^{-1} $Å^{-1}$. The minimized structure had an outer radius of 162.6 Å from the center of the icosahedral symmetry and an inner radius of 106.5 Å.

The minimized coordinates were put into the central cell, and calculations by the method described earlier in this article were started. A region named the water zone was defined as a shell-like volume with outer radius r_{out} and inner radius r_{in} of 99.0 and 170.0 Å, respectively. The empty space of the water zone was filled with additional water molecules, whose coordinates were taken from the AMBER4 wat216.dat file.[13] Water molecules outside the water zone were omitted. Further, water molecules too near (within 1.0 Å) any side plane of the cell and those making short contacts with proteins or with the water molecules contained in the 4RHV file were omitted. The icosahedral symmetry was considered in the short contact check, and the criterion of short contact was a distance of 2.2 Å between nonhydrogen atoms. In total, 3371 water residues (10,113 atoms) were added (a water molecule is counted as a residue), and the total number of atoms in the simulation was increased to 18,637 (4449 residues).

A biharmonic, square-well potential, E_{water}, was added to prohibit evaporation of water as follows:

$$E_{water} = \begin{cases} K_{water} \times (r - r_{out})^2 & (r_{out} < r) \\ 0 & (r_{in} \le r \le r_{out}) \\ K_{water} \times (r - r_{in})^2 & (r < r_{in}) \end{cases} \quad (13)$$

where K_{water} is the force constant of 1.0 kcal mol^{-1} Å^{-2}.

Because displacement of water molecules can be large, they may travel out of the nine cells shown in Figure 2. In such cases, technical problems would be encountered in the simulation because our program is not yet equipped with all the 60 rotation matrices. Therefore, when a water molecule leaves the central cell, it is replaced using the equation

$$\mathbf{x}(k_0)' \leftarrow \mathbf{R}[-\mathrm{cl}(k_0)] \cdot \mathbf{x}(k_0) \quad (14)$$

where the symbol $\leftarrow$ indicates replacement. The preceding equation effects a replacement of the protomer coordinates and is different from eq. (5), which shows the relationship between the protomer coordinates and the cell coordinates. Equation (14) was not applied to protein residues, whose displacement is small. Because water molecules are not connected by any covalent bonds to other residues, no problems arise from eq. (14). The preceding replacement was performed every 20 steps.

The empirical force field energy was minimized under rotational boundary conditions with the positional constraint of 100.0 kcal mol^{-1} Å^{-2}, which was applied to all the nonhydrogenic atoms except the acetyl groups and the additional water molecules. The dielectric constant and the border cutoff were 1.0 and 13.0 Å, respectively. Energy minimization was continued until the rms gradient became 0.7 kcal mol^{-1} Å^{-1}.

A molecular dynamics simulation of 1 ps was carried out with a timestep of 0.001 ps under rotational boundary conditions with the positional constraints of 10.0 kcal mol^{-1} Å^{-2}. The temperature of the initial random velocity was 100 K. Velocity scaling[14] was used to increase the temperature to 300 K with a relaxation time of 1.0 ps.

Finally, a molecular dynamics calculation of 60 ps under rotational boundary conditions was carried out without constraints, starting from the coordinates and the velocities of the final step of the preceding constrained simulation. The temperature relaxation time was changed to 0.1 ps, while other simulation conditions were kept the same.

Molecular dynamics simulation of an isolated protomer was also calculated for comparison. No water molecules were included (calculation *in vacuo*). Other simulation procedures were the same as those mentioned earlier, including a dielectric constant of 4.0.

The computers used were NEC EWS4800/220 and EWS4800/330. Both are inexpensive workstations with cataloged speeds of 33 MIPS and 132 MIPS, respectively, and the former has large cache memory.

Results

Figure 1 shows the minimized structure of the rhinoviral capsid protomer under rotational boundary conditions. Water molecules were distributed spherically around the protein structure.

Figure 4 shows the final snapshot of the 60-ps simulation. The surface of the water was deformed from the spherical shell shape because of water motion in the simulation, whereas the structure of protein was not greatly changed. The conformation

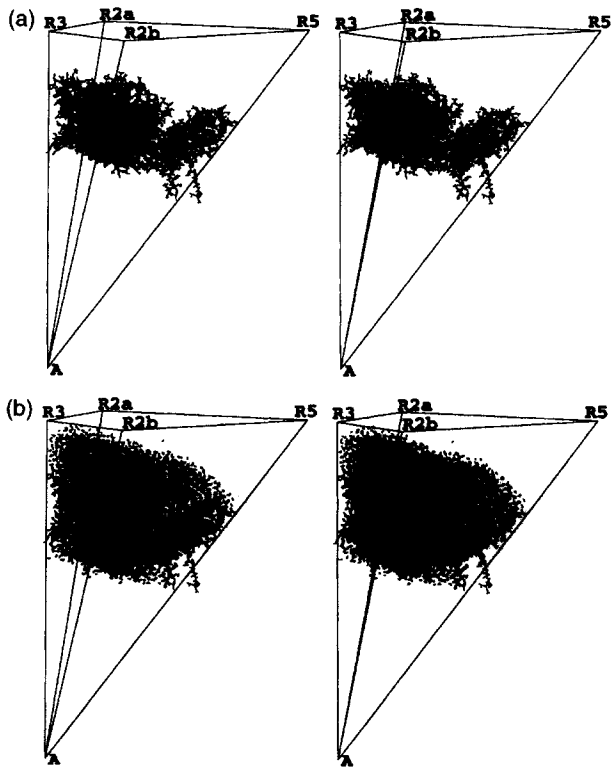

FIGURE 4. Snapshot at 60 ps of the molecular dynamics simulation with icosahedral symmetry. (a) Water molecules not shown. (b) Water molecules shown.

of the arm winding along the fivefold axis (A-R5) was well conserved, as shown in Figure 4. This arm is the amino terminus of VP3, which interacts with four other images to make an inwardly projecting twisted tube.

The conservation of the structure was significant when compared with the final snapshot of the molecular dynamics simulation of an isolated protomer (shown in Fig. 5). Many of the sidechains, loops, and strands were bent onto the protein body in Figure 5. The whole protein was made to have a more compact surface, and the VP3 arm was also completely bent (Fig. 5).

As shown in Figure 6, the rms deviations from the minimized structure increased much more slowly in the icosahedral symmetry simulation compared to the isolated protomer, although full equilibration was observed for neither. The final rms deviation in the simulation under rotational symmetry boundary conditions was 2.0 Å with respect to the starting energy-minimized structure, and that of the isolated protomer simulation was 4.9 Å. One of the causes of this larger deformation of the isolated protomer simulation was, of course, the absence of explicit water molecules. Another possible cause could have been neglect of interprotomer interaction. It is not surprising that the structure of a protomer in a capsid is different from that in the isolated protein. The bending of the VP3 arm onto the protein body (Fig. 5) was clearly a result of this neglect. Comparison with a calculation of an isolated protomer with explicit water molecules under conventional periodic boundary conditions would help explain which cause is more important. Because such a simulation requires a very large box of periodic boundary, such results will be presented elsewhere.

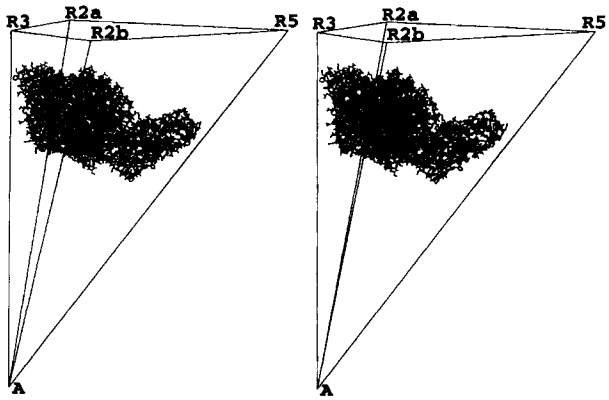

FIGURE 5. Snapshot at 60 ps of the molecular dynamics simulation of an isolated protomer in vacuo.

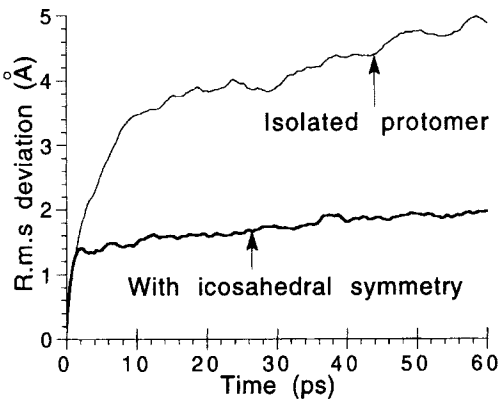

FIGURE 6. Time profile of the rms deviation of the main chain atoms (N, C_α, C, and O) from the energy-minimized starting structure. Bold and thin lines denote simulation in the icosahedral symmetry and that of an isolated protomer in vacuo, respectively.

Figure 7 shows *B* factors of the C_α atoms calculated from the final 10 ps of the calculations. The positions of most peaks were similar to those from X-ray analysis. The *B* factors for the amino termini were often larger in the simulation than in the X-ray analysis. This result is expected, because the amino termini are known to interact with the nu-

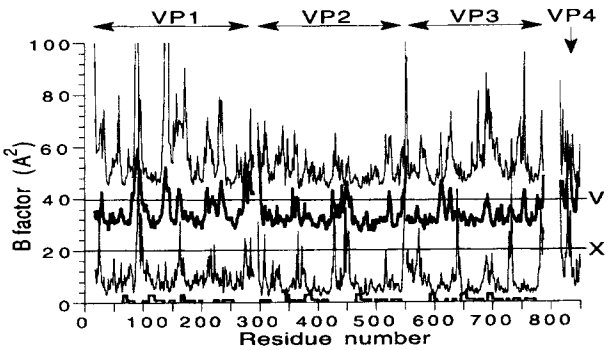

FIGURE 7. *B* factors of the C_α atoms from the simulation with icosahedral symmetry (lower), from the simulation of an isolated protomer in vacuo (upper), and from the X-ray analysis of the 4RHV file (ref. 1) (bold). To avoid overlapping these three curves, the latter two (upper and bold) are shifted upward by 40 and 20 Å, respectively. Lines *V* and *X* are the baselines for the upper and bold curves, respectively. The lowest line in bold denotes parts of α-helices (tall) and β-sheets (short). The sequential numbers of residues follow the style of the 4RHV file. The *B* factors from the simulation are calculated from the apparent mean square atomic displacement in 41 structures of the final 10 ps. The *B* factors are not drawn for the C_α atoms whose coordinates were not determined by X-ray analysis.

cleotide core,[1] which was omitted in the simulation even though it possibly stabilizes the capsid structure. When compared with the isolated protomer simulation, the B factors from the simulation under rotational symmetry boundary conditions were smaller and showed a plot more similar in shape to that obtained by X-ray analysis.

Table IV shows an energy decomposition. The intercell nonbonded interaction was about one tenth of the intracell nonbonded interaction but large enough to control the structure and motion of both protein and water.

The neighbor atom pair list was generated with the residue-based cutoff of 8 Å, as described earlier. The number of residue distances calculated for neighbor list generation is approximately $N_R \times N_R/2$ when N_R is very large. N_R is the number of residues of a protomer (i.e., 4449), so $N_R \times N_R/2 = 9.9 \times 10^6$ for intracell and 3.7×10^6 for intercell nonbonded interactions. The number of neighbor atom pairs selected was 2.8×10^6 for intracell and 0.7×10^6 for intercell nonbonded interactions. The CPU time for a 10-ps simulation was 14 days with an EWS4800/220 workstation, and that for a 50-ps simulation was 27 days with an EWS4800/330 workstation. Longer calculations, more detailed analysis, and biological discussion will be presented elsewhere.

TABLE IV.
Decomposition of Potential Energy.[a]

	Min[b]	Final[c]
Total Potential Energy	−64329.8	−65470.3
Intracell Nonbonded Interaction		
Electrostatic	−94874.9	−97059.8
Lennard-Jones	−2264.0	−1592.0
H bond	−487.7	−799.0
Intercell Nonbonded Interaction		
Electrostatic	−3901.0	−6021.0
Lennard-Jones	−2264.0	−496.6
H bond	−33.1	−62.6
Other Potential Energy		
Bond	2261.5	5205.2
Angle	1685.4	2768.1
Torsion	2062.3	2010.2
1-4vdw	2089.1	1768.0
1-4el	27225.4	28190.6
Improper	267.1	613.3
Positional constraint	2223.0	—
Constraints, E_{water}, for water	0.7	5.2

[a] Units in kcal mol^{-1}.
[b] Minimization under rotational symmetry boundary conditions.
[c] Final structure of the simulation under rotational symmetry boundary conditions. Temperature was 306 K and the kinetic energy was 17013.0 kcal mol^{-1}.

Discussion

Neighbor list generation was greatly accelerated by the method of rotational symmetry boundary conditions and the border residue flags developed in this study. As presented earlier, the number of residue distances calculated for the neighbor list generation was $9.9 \times 10^6 + 3.7 \times 10^6 = 13.7 \times 10^6$ in total. This is only 1.4 times the value of $N_R \times N_R/2$ for neighbor list generation in the conventional isolated protomer simulation. Consequently, the large computational burden for the neighbor list generation described in the Introduction was decreased approximately from 119 times or 17 times to only 1.4 times that of the conventional isolated protomer simulation method. Use of our neighbor list generation method in capsid simulations is only a little slower than for standard protein simulations.

Once the neighbor list is prepared, calculation of the nonbonded energy itself is a little faster than the conventional periodic boundary simulation because there are no interactions for the truncated inner and outer regions of the water zone of the capsid. The total CPU time necessary for capsid simulations with our method is comparable to that for conventional protein simulations. Comparing our experience of the periodic boundary simulation of HIV-1 protease,[15] each step took 110 s in the HIV-1 simulation (12,375 atoms), whereas each step in the present study (18,637 atoms) took 120 s on the same EWS4800/220. Although strict comparison of speed is, of course, difficult, it is certain that our development of rotational symmetry boundary conditions enables practical entire capsid simulations on inexpensive computers.

Symmetry assumptions are accompanied by disadvantages with regard to asymmetrical properties. For example, it is difficult to study global asymmetrical deformation, such as the uncoating process of viral capsids. It is also difficult to calculate local asymmetry. For example, the positions of

the three water oxygens HOH-1, HOH-66, and HOH-228 in the 4RHV file are almost on the fivefold axis A-R5, the threefold axis A-R3, and the twofold axis A-R2b, respectively (Fig. 1). These oxygens make short contacts with their own images, causing energies to be too high. Thus, we omitted these three water molecules, as discussed earlier. Although a slight displacement of the oxygens from the axes could eliminate these short contacts, we believe that it is necessary to interpret the positions of these oxygens as on the axes, because the occupancies are smaller than 1.0. A water molecule has, however, two hydrogen atoms, the positions of which can never be symmetrical around the axes. Thus, these water molecules cannot be included in the calculations under our symmetry assumptions. The difficulties concerning the asymmetrical properties can be clarified through comparison with calculations without symmetry assumptions.

Our molecular dynamics simulation of the rhinoviral capsid lacked the nucleotide core structure, which has not been determined yet by X-ray analysis for this class of virus. Furthermore, the core structure is not icosahedrally symmetrical. This lack of nucleotide core causes, of course, many problems, such as the large B factor of the amino termini which interact with the nucleotide core, as described earlier. Thus, properties of the models that are strongly related to the nucleotides cannot be considered under the present symmetry assumptions. The rhinoviral capsid structure should, however, be stable without the nucleotide core because picornaviruses generally produce natural empty capsids which contain no nucleotide core.[16] Furthermore, the biharmonic square-well potential added to water molecules in our calculations acts as a force to help maintain the capsid structure. In fact, sufficient stability in the icosahedral symmetry was shown in Figure 6. Therefore, molecular dynamics simulation with symmetry can yield important information about the capsid structure.

It is clear that the method presented here is widely applicable to any crystallographic or noncrystallographic symmetry. For example, a unit lattice of a protein crystal is often composed of several protein molecules, which have identical conformations and are related to each other by a combination of rotation and linear translations. Although conventional periodic boundary conditions are not applicable to such types of symmetries, the method developed in this study is expected to become a powerful tool for studies of such symmetries.

Conclusions

The rotational symmetry boundary conditions were implemented in the APRICOT program to make simulations of the icosahedrally symmetrical capsids. The new notations, treatment, and equations were proposed for practical calculation under rotational symmetry boundary conditions. The use of border residue flags was also introduced to accelerate neighbor atom pair list generation. Using this development, the 60-ps simulation of a rhinoviral capsid was calculated with inexpensive workstations. This is the first molecular dynamics simulation of an entire viral capsid using rotational symmetry boundary conditions. Although this development is not applicable to global asymmetrical conformational changes or to the local asymmetry around the rotation axes, it may be used to clarify the symmetrical and asymmetrical properties of large molecular assemblies. This development is applicable to any crystallographic or noncrystallographic symmetry.

Acknowledgments

We express appreciation to Drs. Kenshu Kamiya, Teruyo Yoneda, and Junichi Higo for their valuable advice.

References

1. (a) M. G. Rossmann, E. Arnold, J. W. Erickson, E. A. Frankenberger, J. P. Griffith, H. J. Hecht, J. E. Johnson, G. Kamer, M. Luo, A. G. Mosser, R. R. Rueckert, B. Sherry, and G. Vriend, *Nature*, **317**, 145 (1985); (b) E. Arnold and M. G. Rossmann, *Acta Cryst.*, **A44**, 270 (1988).
2. S. C. Harrison, In *Virology*, 2nd ed., B. N. Fields, D. M. Knipe, R. M. Chanock, M. S. Hirsch, J. L. Melnick, T. P. Monath, and B. Roizman, Eds., Raven Press, New York, 1990, p. 37.
3. T. Cagin, M. Holder, and B. M. Pettitt, *J. Comp. Chem.*, **21**, 627 (1991).
4. For example, see M. P. Allen and D. J. Tildesley, *Computer Simulation of Liquids*, Oxford University Press, New York, 1987, and references cited therein.
5. M. Kitazawa, Master's thesis, School of Pharmaceutical Sciences, Kitasato University, Tokyo, Japan, March, 1993 (in Japanese).
6. T. P. Lybrand and J. A. McCammon, *J. Comp.-Aided Mol. Design*, **2**, 259 (1988).

7. R. C. Wade and J. A. McCammon, *J. Mol. Biol.*, **225,** 679 (1992).
8. W. F. Lau and B. M. Pettitt, *J. Med. Chem.*, **32,** 2542 (1989).
9. B. R. Brooks, R. E. Bruccoleri, B. D. Olafson, D. J. States, S. Swaminathan, and M. Karplus, *J. Comp. Chem.*, **4,** 187 (1983).
10. S. Yoneda and H. Umeyama, *J. Chem. Phys.*, **97,** 6730 (1992).
11. S. J. Weiner, P. A. Kollman, D. A. Case, U. C. Singh, C. Ghio, G. Alagona, S. Profeta, Jr., and P. Weiner, *J. Am. Chem. Soc.*, **106,** 765 (1984).
12. W. L. Jorgensen, J. Chandrasekhar, J. D. Madura, R. W. Impey, and M. L. Klein, *J. Chem Phys.*, **79,** 926 (1983).
13. D. A. Pearlman, D. A. Case, J. C. Caldwell, G. L. Seibel, U. C. Singh, P. Weiner, and P. A. Kollman, *AMBER 4.0*, University of California, San Francisco, 1991.
14. H. J. C. Berendsen, J. P. M. Postma, W. F. van Gunsteren, A. DiNola, and J. R. Haak, *J. Chem. Phys.*, **81,** 3684 (1984).
15. S. Yoneda, N. Yamashita, and H. Umeyama, *The 20th Symposium on Structure Activity Relationships*, Kyoto, Japan, September 27, 1992 (oral presentation in Japanese).
16. R. R. Rueckert, In *Virology*, 2nd ed., B. N. Fields, D. M. Knipe, R. M. Chanock, M. S. Hirsch, J. L. Melnick, T. P. Monath, and B. Roizman, Eds., Raven Press, New York, 1990, p. 507.